Camera Calibration Using Composed Cubic Splines

Abstract

Camera calibration is a process whereby the geometric characteristics of a specific camera are determined. It is performed in order that the photograph obtained can be used to produce accurate measurements.

This paper presents a simple and accurate model to extract the optical characteristics (intrinsic parameters) and the 3D position and orientation of the camera (extrinsic parameters) based on image coordinate measurements of targets of known 3-D position. The proposed algorithm is divided into two major steps. First, the behaviour of a grid of projected lines is studied and the needed local corrections are applied. Such corrections are calculated using Composed Cubic Splines. This function covers radial, decentering and prism distortions. It gives a more realistic model of distortion which is represented as a composed surface. Then, calibration parameters are estimated using a pinhole model based on the minimization of a linear criterion relating the 3D coordinates of the targets with their 2D image projections.

Key words

Camera calibration, lens distortions**,** pinhole model, Composed Cubic Splines.

1- Introduction

Camera calibration is particularly crucial in applications such as the construction of 3D models and the dimensional measurements of a given object. Accurate calibration is necessary in computer vision and photogrammetry.

Generally, the calibration of a camera is the determination of the relationship between 2D pixel coordinates and 3D object coordinates. It fixes the parameters describing the projection of a three-dimensional scene onto a two-dimensional surface. These

parameters describe the internal characteristics of a camera (focal length, pixel size, distortion coefficients and pixel coordinates of principal point) and external parameters (position and orientation of the camera frame relative to a given object coordinate system).

Existing camera calibration techniques can be classified into three methods (Cramer 2004). The first method is laboratory calibration, used to verify the validity of camera parameters and it is repeated within certain time intervals. A second method, called on-site calibration, is performed by using targets positioned beside the object of interest. Camera calibration parameters and object space position are estimated simultaneously. A third method, called autocalibration, does not use any calibration object. The internal and external parameters are estimated by using image information only (Zhang et al. 2008, Ha and Kang 2005).

Several techniques are based on image observation of points of known 3-D coordinates (Ramalingam et al. 2006) or shape like circles (Mateos 2000) and ellipses (Zhang et al. 2005). They involve determining the mathematical model expressed in a perspective transformation matrix. Different techniques exist for the computation of that matrix and may be classified into two categories: linear techniques which use the minimization of a linear criterion relating 3D points coordinates and their 2D image projections (Tsaï 1987); and non-linear optimisation techniques which address lens distortions and minimize the errors between observed and calculated parameters using iterative algorithms (Weng 1992).

The calibration technique that we present is of the second method type: calibration is achieved using targets of known 3-D coordinates. For the given setup, our algorithm uses direct and indirect techniques to estimate intrinsic and extrinsic parameters. A Composed Cubic Splines function calculates distortions in order to obtain a true pinhole model. The parameters of this function control more complex forms of distortion. The interpolation formula gives an accurate result both in terms of parameters and errors. The development of this new method has been motivated by the increased potential of digital cameras for

accurate measurements and by the more complex and less stable geometry that these cameras involve.

The following Section describes the calibration procedure, presenting the linear method for solving parameters and following with the application of nonlinear optimization. Section 3 presents three models that have been used to calculate the distortion function. Section 4 studies different methods of image data extraction. Section 5 reports experimental results of a real case of calibration. Finally, the conclusion and discussion are presented in Section 6.

2- Calibration procedure and mathematical models

The pinhole model is the most frequently used model for camera calibration. It is based on the collinearity principle. It is characterized by three transformations (Figure 1):

- Transformation of 3-D scene coordinates (*X,Y,Z*) in 3-D camera coordinates (*x,y,z*).
- Projection of 3-D point coordinates (*x,y,z*) in 2D image point coordinates (*x',y'*) centered in O (*x'* et *y'* axis are parallel to x and y).
- Transformation of coordinates (*x',y'*) in millimetres to coordinates (*u,v*) in pixels.

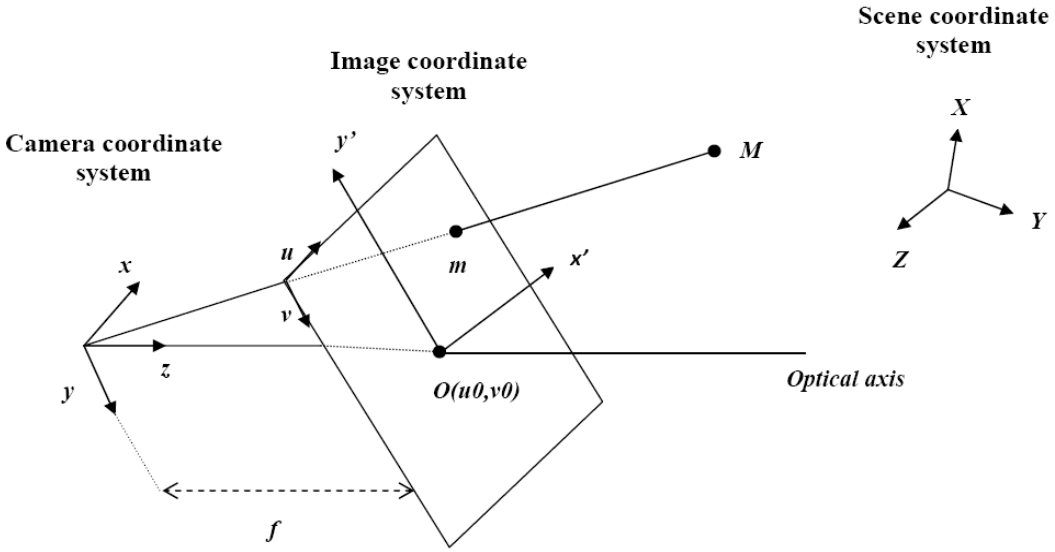

Figure 1: Geometrical Model

The relationship between the coordinates of a space point *(X,Y,Z)* and its image projection *(u,v)* is given by the following matrix equation in the homogeneous coordinate system :

$$\begin{pmatrix} ku \\ kv \\ k \end{pmatrix} = \begin{pmatrix} \alpha_u & 0 & u_0 & 0 \\ 0 & \alpha_v & v_0 & 0 \\ 0 & 0 & 1 & 0 \end{pmatrix} . \begin{pmatrix} r_{11} & r_{12} & r_{13} & \mathrm{t_x} \\ r_{21} & r_{22} & r_{23} & \mathrm{t_y} \\ r_{31} & r_{32} & r_{33} & \mathrm{t_z} \\ 0 & 0 & 0 & 1 \end{pmatrix} . \begin{pmatrix} X \\ Y \\ Z \\ 1 \end{pmatrix}. \quad (1)$$

Or:

$$\begin{pmatrix} ku \\ kv \\ k \end{pmatrix} = \begin{pmatrix} \alpha_u & 0 & u_0 & 0 \\ 0 & \alpha_v & v_0 & 0 \\ 0 & 0 & 1 & 0 \end{pmatrix} . \begin{pmatrix} R & T \\ 0 & 1 \end{pmatrix} \begin{pmatrix} X \\ Y \\ Z \\ 1 \end{pmatrix}, \quad (2)$$

where:

- (u_0,v_0): the pixel coordinates of principal point O which is the intersection of the optical axis with the image plan;
- (α_u,α_v): scale factors of the image axes *u* and *v* (in pixels);
- *R* and *T:* rotation and translation between scene and camera coordinate systems;
- u_0,v_0, α_u and α_v: the intrinsic camera parameters;
- *R* and *T*: the extrinsic camera parameters.

2.1 Linear parameters estimation

Equation 2 can be written as follows:

$$\begin{pmatrix} ku \\ kv \\ k \end{pmatrix} = M . \begin{pmatrix} X \\ Y \\ Z \\ 1 \end{pmatrix} . \quad (3)$$

M, the projection matrix, being:

$$M = \begin{pmatrix} m_{11} & m_{12} & m_{13} & m_{14} \\ m_{21} & m_{22} & m_{23} & m_{24} \\ m_{31} & m_{32} & m_{33} & m_{34} \end{pmatrix}.$$

- **First method: constraint $m_{34}=1$**

The parameters of matrix M can be estimated using the known object coordinates (X_i,Y_i,Z_i) of targets and their image projection (u_i,v_i). When $m_{34}=1$, the equation of point i is:

$$\begin{pmatrix} \vdots & \vdots & \vdots & \vdots & \vdots & \vdots & \vdots & \vdots & \vdots & \vdots & \vdots \\ \mathrm{X_i} & \mathrm{Y_i} & \mathrm{Z_i} & 1 & 0 & 0 & 0 & 0 & -\mathrm{u_i X_i} & -\mathrm{u_i Y_i} & -\mathrm{u_i Z_i} \\ 0 & 0 & 0 & 0 & \mathrm{X_i} & \mathrm{Y_i} & \mathrm{Z_i} & 1 & -v_{\mathrm{i_i}}\mathrm{X_i} & -v_{\mathrm{i_i}}\mathrm{Y_i} & -v_{\mathrm{i_i}}\mathrm{Z_i} \\ \vdots & \vdots & \vdots & \vdots & \vdots & \vdots & \vdots & \vdots & \vdots & \vdots & \vdots \end{pmatrix} \begin{pmatrix} m_{11} \\ m_{12} \\ m_{13} \\ m_{14} \\ m_{21} \\ m_{22} \\ m_{23} \\ m_{24} \\ m_{31} \\ m_{32} \\ m_{33} \end{pmatrix} = \begin{pmatrix} \vdots \\ \mathrm{u_i} \\ \mathrm{v_i} \\ \vdots \end{pmatrix}. \quad (4)$$

Equation 4 can be solved by the least-squares technique. The equation being of the form $AM = \mathrm{B}$, the solution is given by minimizing the sum of the squared difference between left and right sides:

$$\mathrm{M} = (\mathrm{A^t A})^{-1}\mathrm{A^t B}. \quad (5)$$

- **Second method: constraint $m_{31}^2 + m_{32}^2 + m_{33}^2 = 1$**

Faugeras and Toscani (Faugeras and Toscani 1987) proposed the constraint $m_{31}^2 + m_{32}^2 + m_{33}^2 = 1$. This method has shown to provide a good estimate for the projection matrix.

The disadvantage of linear approach, however, is that it cannot incorporate lens distortion. For that reason, the photogrammetry community has proposed using a nonlinear estimation method (Weng et al. 1990).

2.2 Nonlinear parameters estimation

The pinhole model is just an approximation referring to a projection in an ideal imaging system. A better suited model must take into account the displacement caused by radial and tangential distortions. In that case, estimation of the camera parameters requires applying an iterative algorithm.

The first step is to use a linear method to get an initial solution for the projection matrix. This provides initial parameters which are used in an iterative algorithm (Equation 6), minimizing the residuals between the initial model and the N observations (Weng et al. 1990).

$$V = \sum_{i=1}^{N}(u_i - u'_i)^2 + \sum_{i=1}^{N}(v_i - v'_i)^2, \quad (6)$$

where:

- (u_i, v_i): the undistorted or ideal image coordinates,
- (u'_i, v'_i): the distorted or true image coordinates.

The main advantage of this approach is that distortion parameters can be estimated .

3- An approach for distortion calibration

As a first step in the computation of undistorted image coordinates, for the pinhole model, a distortion estimation has to be performed at different points for the projected image. Then, using a Composed Cubic Splines function, the pixel shift, at every point, can be computed.

Distortion displacement is generally modeled using polynomial approximation (Zollener 2003, Perse and Kovacic 2002). In usual photogrammetry practice, only radial distortion, generally, is considered because its more significant influence on the image geometry. However, if a better idea of the camera optical quality is needed, others components, such as decentering distortion, have to be taken into account. Thus a method is needed that can model the more complex correction procedure. Equation 7 models the application of the correction:

$$\begin{cases} u_i = u'_i + \Delta u_i \\ v_i = v'_i + \Delta v_i \end{cases}, \quad (7)$$

where $(\Delta u_i, \Delta v_i)$ are the relative corrections to the distorted coordinates, giving the corrected values in the *u* and *v* directions.

Existing literature presents many polynomial distortion models (Ma et al. 2003), with performance varying in function of the accuracy needed or of the magnitude of radial distortion.

In the new model presented here, the behaviour of a grid of projected lines has been studied in order to provide the needed local corrections. The accurate model is computed using many control points. This model takes into account radial and tangential distortion and calculates the corrections needed to obtain a true pinhole model.

3.1 Model 1: Global modeling using nonlinear method

In the method of nonlinear global modeling, presented hereafter, the function F (Equation 8) is designed to minimize the errors, for the n observed points, between their observed values (U_i, V_i) and the corresponding (u_i, v_i), computed after estimating the camera parameters. Using an iterative algorithm, the following function has to be minimized:

$$F = \sum_{i=1}^{n}(u_i - U_i)^2 + \sum_{i=1}^{n}(v_i - V_i)^2. \quad (8)$$

3.2 Model 2: Correction of line deformation

Distortion causes straight lines to be projected as curved lines. In Method 2, the distorted vertical and horizontal lines of a grid are transformed into straight lines. Starting with a photograph of a grid (Figure 2), the operation consists of:

- Finding the grid intersection points,
- Forming the equations of the lines:

$$v = a_i * u + b_i \quad (i \text{ is the horizontal line number}). \quad (9)$$

$$v = a_j * u + b_j \quad (j \text{ is the vertical line number}). \quad (10)$$

The error functions F_i and F_j that define the square error in horizontal line *i* and vertical line *j*, p and q being the number of horizontal and vertical lines respectively, are:

$$\begin{cases} F_i = \sum_{m=1}^{p} (v_{mi} - a_i * u_{mi} - b_i)^2 \\ F_j = \sum_{n=1}^{q} (v_{nj} - a_j * u_{nj} - b_j)^2 \end{cases} \quad (11)$$

The total error function can be written

$$F = \sum_{i=1}^{p} F_i + \sum_{j=1}^{q} F_j, \quad (12)$$

which is minimized by least squares.

- The new intersections of the horizontal and vertical lines computed by least squares are the true grid locations. The new coordinates, compared to the initial ones, give the distortion at each point.

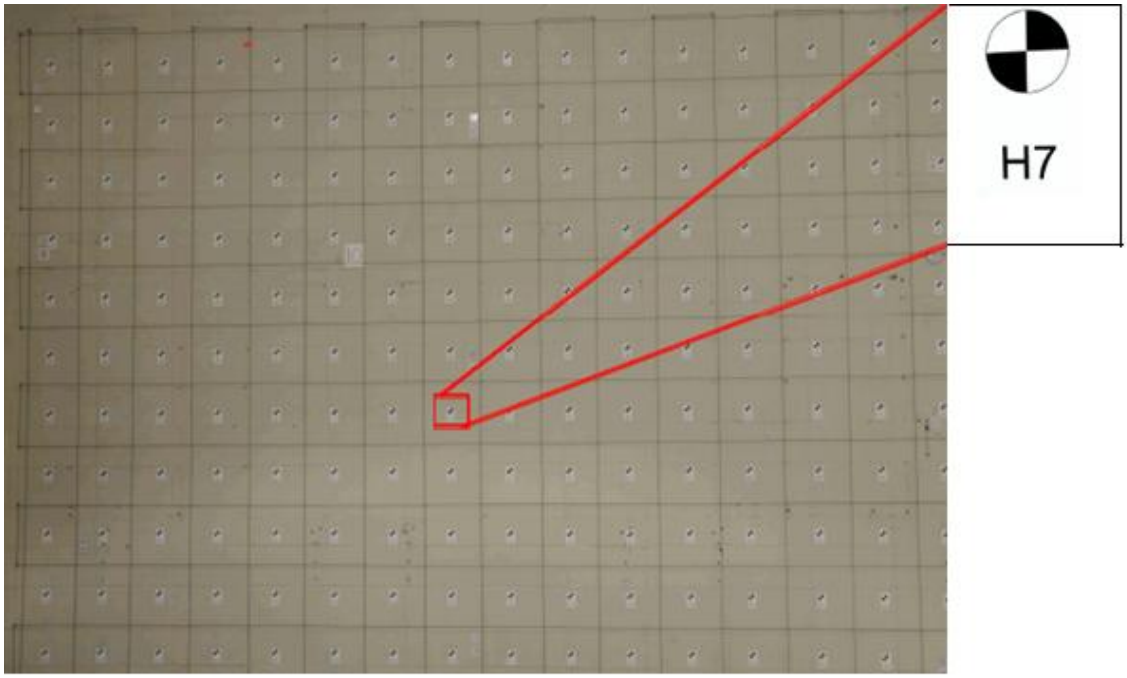

Figure 2: Grid and Calibration Target

3.3 Model 3: Grid correction

A similar procedure can be used to measure the distortion transforming grid straights lines into curves.

The method is based on a concept developed by Brand et al. (Brand et al. 1993), except that only intersection point corrections are computed. It consists of the following steps:

- Observing a gird to delineate the areas to which a correction must be applied locally.
- Finding the location of the intersection.
- Computing the ideal coordinates for these points using the pinhole model. In a virtual reference, points are positioned in $(0,0), (0,1), \ldots (i,j) \ldots (n,m)$.
- Transforming each distorted rectangle of the grid image into an ideal rectangle in the virtual reference using projective transformation (4 points are selected at the corners of the image, for which no correction is applied).
- Generalizing this transformation to all points by bilinear interpolation.
- Applying an inverse transformation to find pixel coordinates.

3.4 Distortion computed by a Composed Cubic Splines function

A Composed Cubic Splines function models a theoretical form using a combination of linear terms. Generally, it is used to generate data fitting. In the present application, it is used to interpolate in the case of unequally spaced data points and determine the distortion for each pixel.

Using this process, a unique continuous function models the distortion at every point of the image. The function has the following form:

$$s(x,y) = \sum_{i=1}^{n} a_i \sqrt{(x-x_i)^2 + (y-y_i)^2}^3 \quad , \qquad (13)$$

where :

$$\begin{cases} n: nomber\ of\ knots \\ a_i: knot\ parameter \\ (x_i, y_i): coordinates\ of\ knot\ i \\ (x,y): coordinates\ of\ any\ point \end{cases} .$$

The usual methods give information for the distortion function, by polynomial approximation, in 2 or 3 coefficients. Generally, only radial distortion is estimated, the tangential being considered negligible. Using Composed Cubic Splines, the information

obtained contains much more coefficients (150 in the present case), from which an appreciable accuracy gain can necessary be expected.
An additional advantage comes from the fact that the nodes can be placed anywhere on the surface (Plante 1999).

The distortion can be computed at any point of position *(u,v)*, the surface image being modeled by a linear combination of terms, as shown by Equation 14.

$$\begin{cases} \Delta u(u,v) = \sum_{i=1}^{n} a_i \sqrt{(u-u_i)^2 + (v-v_i)^2}^3 \\ \Delta v(u,v) = \sum_{i=1}^{n} b_i \sqrt{(u-u_i)^2 + (v-v_i)^2}^3 \end{cases}, \tag{14}$$

where:

$(\Delta u, \Delta v)$: Local Correction in order to perform pinhole

(u, v) : Coordinates of a pixel in the image,

(u_i, v_i) : Coordinates of knot i,

(a_i, b_i) : Parameters of knot i.

The following matrices have to be solved:

$$D^3 a = \Delta u \tag{15}$$

and

$$D^3 b = \Delta v\ , \tag{16}$$

where :

$$D^3 = \begin{pmatrix} 0 & \sqrt{(u_1-u_2)^2+(v_1-v_2)^2}^3 & \dots & \sqrt{(u_1-u_n)^2+(v_1-v_n)^2}^3 \\ \sqrt{(u_2-u_1)^2+(v_2-v_1)^2}^3 & 0 & \dots & \sqrt{(u_2-u_n)^2+(v_2-v_n)^2}^3 \\ \vdots & \vdots & \ddots & \vdots \\ \sqrt{(u_n-u_1)^2+(v_n-v_1)^2}^3 & \sqrt{(u_n-u_2)^2+(v_n-v_2)^2}^3 & \dots & 0 \end{pmatrix},$$

$$a = \begin{pmatrix} a_1 \\ a_2 \\ \vdots \\ a_n \end{pmatrix},$$

$$b = \begin{pmatrix} b_1 \\ b_2 \\ \vdots \\ b_n \end{pmatrix},$$

$$\Delta u = \begin{pmatrix} \Delta u_1 \\ \Delta u_2 \\ \vdots \\ \Delta u_n \end{pmatrix},$$

$$\Delta v = \begin{pmatrix} \Delta v_1 \\ \Delta v_2 \\ \vdots \\ \Delta v_n \end{pmatrix}.$$

It is also possible to combine the parameters a and b in a matrix ab and corrections Δu and Δv in a matrix $\Delta u \Delta v$, which gives:

$$D^3 ab = \Delta u \Delta v \tag{17}$$

4- Methods for image data extraction

There are different ways of achieving image data extraction. Image data extraction is necessary to establish a correspondence between control points in the object space and their projection in the image. Figure 2 shows a target used for calibration.

The edge pixels of the targets can be determined using any suitable edge detect method. *Hough transform* can be used to detect shapes, such as circles and lines, with sub-pixel accuracy (Ballard 1981).

The centers of projected circles in the image can be determined using three methods:

- **Intersect method:** The method is a least squares computation of the intersection point of two perpendicular diameters (Figure 3).

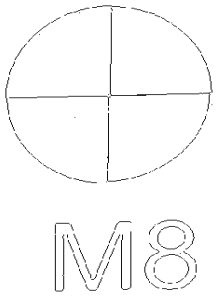

Figure 3: Edge Detection of a Target

- **Circle method:** Given a number n (n≥ 3) of edge pixels on a circle, the least squares solution of Equation 18 determines the coordinates u_0 and v_0 of the target center.

$$\begin{bmatrix} u_1 & v_1 & 1 \\ u_2 & v_2 & 1 \\ \vdots & \vdots & \vdots \\ u_n & v_n & 1 \end{bmatrix} \begin{bmatrix} -2u_0 \\ -2v_0 \\ {u_0}^2 + {v_0}^2 - R^2 \end{bmatrix} = \begin{bmatrix} -{u_1}^2 - {v_1}^2 \\ -{u_2}^2 - {v_2}^2 \\ \vdots \\ -{u_n}^2 - {v_n}^2 \end{bmatrix} \tag{18}$$

The problem can also be solved iteratively using an algorithm similar to the Levenberg-Marquardt method. The accuracy of the results depends on the number of iterations and the number of edge pixels used.

- **Ellipse method:** under the effect of radial and tangential distortions, the perspective projection of a circle is an ellipse (Mateos 2000). The distortion of the circle image depends on the angle and spacing between the object surface (target) and the image plane.

The general equation of a conic in pixel coordinates is:

$$Au^2 + 2Buv + Cv^2 + 2Du + 2Ev + F = 0, \tag{19}$$

which can also be written as:

$$2B'xy + C'y^2 + 2D'x + 2E'y + F' = -x^2 \tag{20}$$

Where *B'=B/A, C'=C/A, D'=D/A, E'=E/A* et *F'=F/A.*

5 edge points are needed to calculate the 5 parameters of the ellipse. The system of equations is the following:

$$\begin{pmatrix} 2u_1v_1 & v_1^2 & 2u_1 & 2v_1 & 1 \\ \vdots & \vdots & \vdots & \vdots & \vdots \\ 2u_nv_n & v_n^2 & 2u_n & 2v_n & 1 \end{pmatrix} \begin{pmatrix} B' \\ C' \\ D' \\ E' \\ F' \end{pmatrix} = \begin{pmatrix} -u_1^2 \\ . \\ . \\ . \\ -u_n^2 \end{pmatrix}. \quad (21)$$

The coordinates (u_0,v_0) of the ellipse center are given by:

$$\begin{cases} Ax_0 + By_0 + D = 0 \\ Bx_0 + Cy_0 + E = 0 \end{cases}. \quad (22)$$

Given the parameters of the Equation 21, the center of ellipse can be determined with accuracy.

5- Experimental results and discussion

Experimentation of the camera calibration procedures was carried at ... The 3-D grid consisted of 339 targets regularly spaced on perpendicular walls, as shown in Figure 4. Different images were acquired with a Nikon D600 at an image resolution of 4288 x 2848 pixels.

Figure 4: 339 targets of calibration object

The camera parameters have been determined using the control points, by application of the different methods presented above. The evaluation is based on the comparison of the residuals after least squares adjustment, each residual being the difference between observed and computed pixel value.

For the determination of the target centers, giving the control points values, the ellipse and circle methods have given closely similar results, and, by comparing the standard deviations, have shown to be the most accurate (Table 1).

Table 1: Residuals and standard deviations for the different methods of image data extraction, in pixels

targets	Comparison Ellipse-circle		Comparison Ellipse-intersection		Comparison Circle-intersection	
	Δu_i	Δv_i	Δu_i	Δv_i	Δu_i	Δv_i
1	0,04	-0,03	0,49	-0,03	0,44	-0,16
2	-0,00	0,01	0,50	0,01	0,51	0,18
3	-0,01	0,05	0,49	0,05	0,49	0,22
4	-0,02	0,02	0,33	0,02	0,36	-0,03
5	-0,00	0,03	0,71	0,01	0,71	-0,26
6	-0,00	0,02	0,89	0,02	0,89	-0,51
7	-0,03	-0,02	0,47	-0,02	0,49	-0,36
8	0,03	0,01	0,30	0,01	0,28	-0,34
9	0,04	0,03	0,74	0,03	0,70	-0,22
10	0,33	-0,70	0,71	-0,69	0,38	-0,09
σ	**0,005**		**0,014**		**0,014**	

5.1 Distortion correction

As a first step in the computation of the distortion function, the correction has been estimated at the different control points using the three methods described in section 3. The coefficients a_i and b_i of Equation 17 have been computed from the results obtained.

The correction vectors of distortion for control points are illustrated in Figure 5, 6 and 7. An example of interpolation using Composed Cubic Splines is shown in Figure 8.

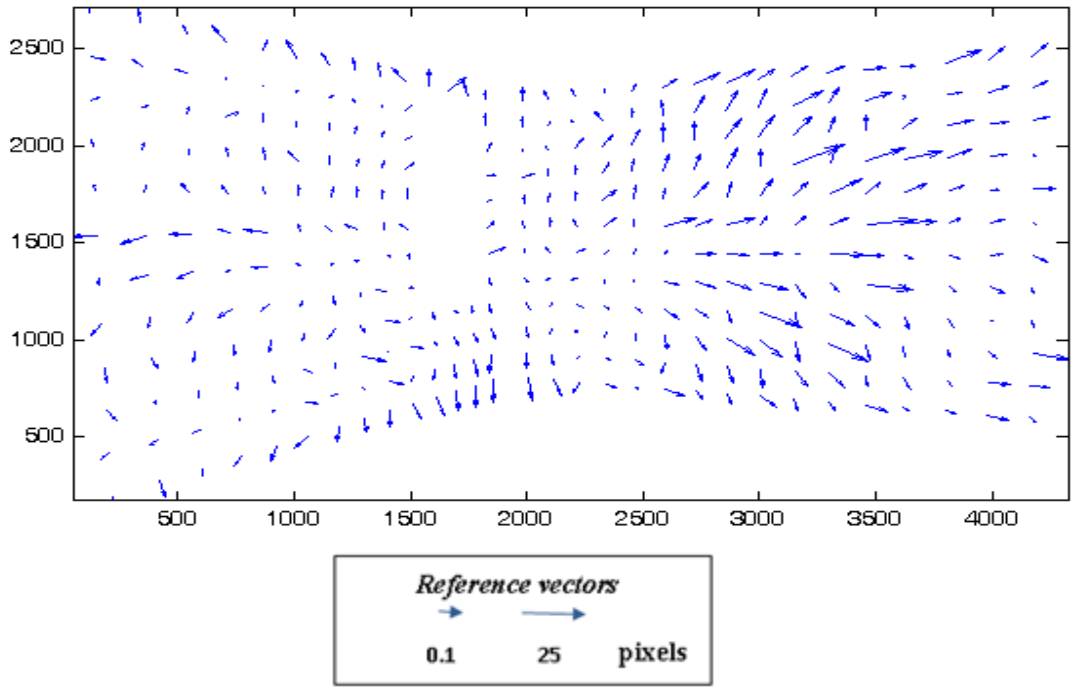

Figure 5: Displacement vectors between distorted image coordinates and undistorted image coordinates (Model 1: Global modeling using nonlinear method)

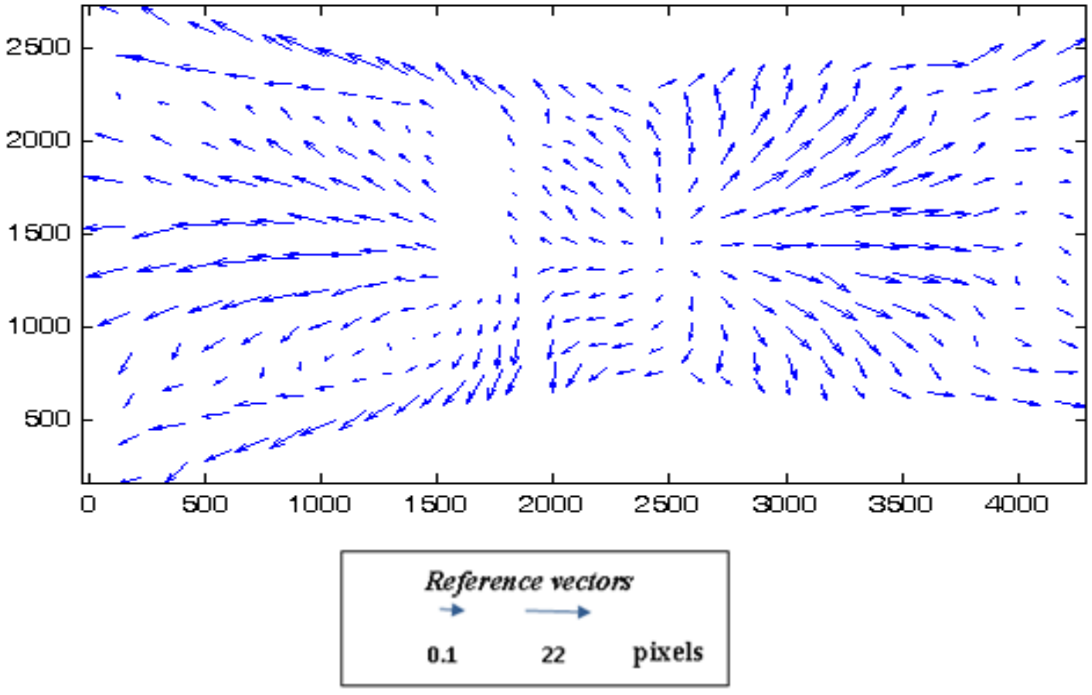

Figure 6: Displacement vectors between distorted image coordinates and undistorted image coordinates (Model 2: Correction of line deformations)

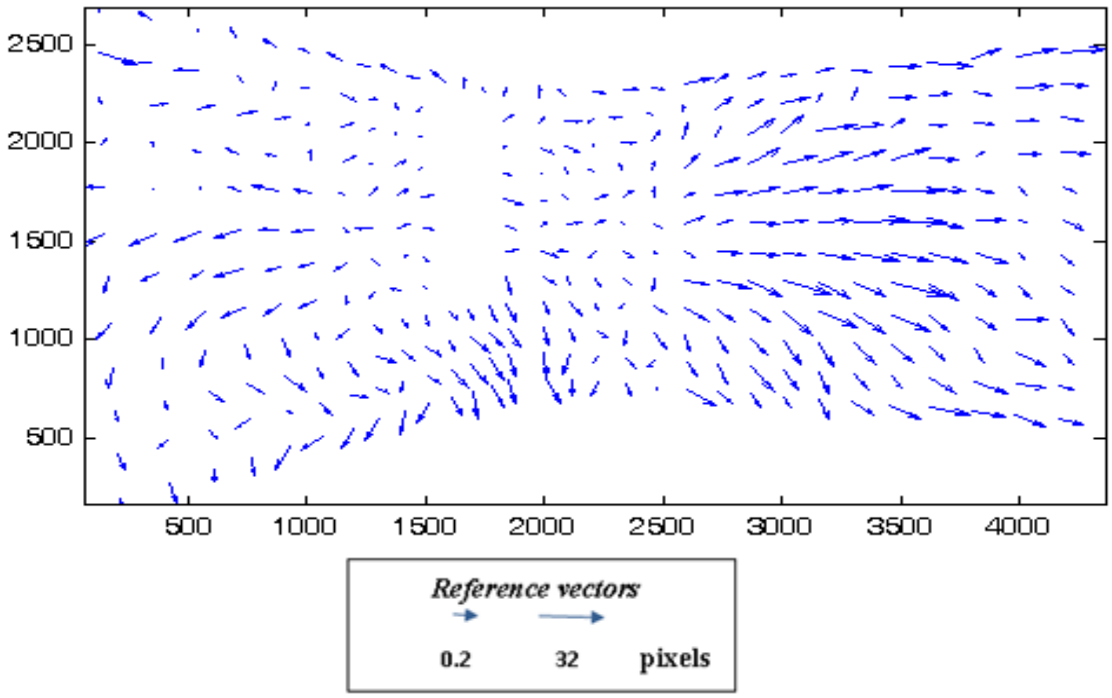

Figure 7: Displacement vectors between distorted image coordinates and undistorted image coordinates (Model 3: Correction of a grid)

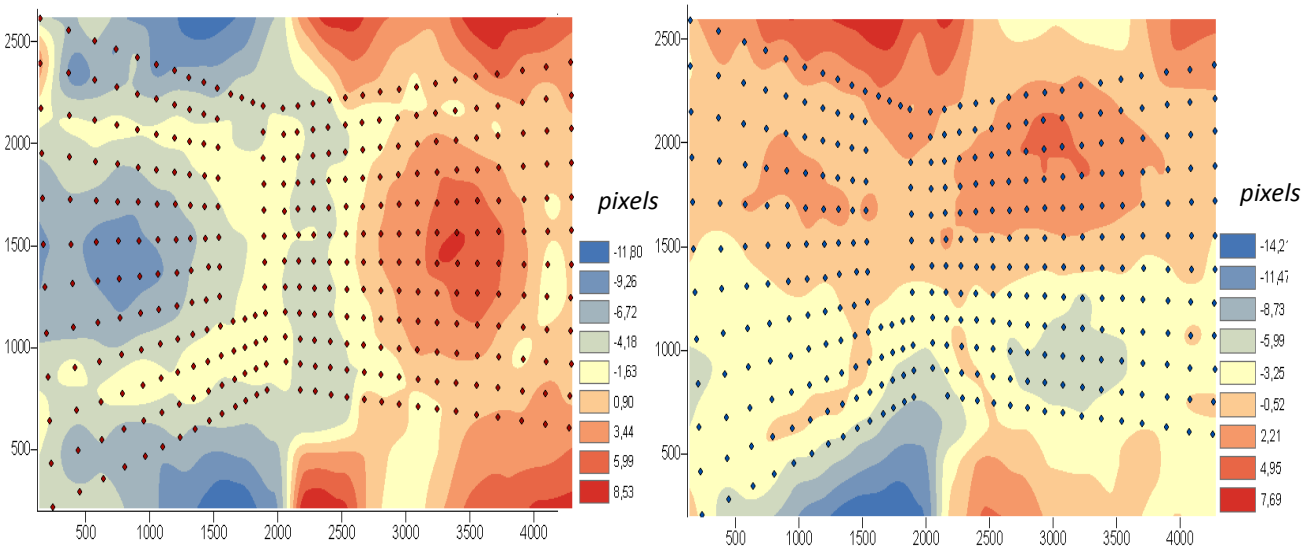

Figure 8: Interpolation of distortion using Composed Cubic Splines

u direction(right) and v direction (left)

The three methods can be compared using function F (Equation 8), by which are evaluated the residual errors between n observed values and their corresponding values given by the different models.

The results indicate that global modeling using nonlinear method (model 1) and correction of line deformation (model 2) are the most accurate. But the grid correction method (model 3) is also an important approach because the deformations of grid lines are shown clearly.

Figure 8 presents the results using Composed Cubic Splines. The results are obtained by fitting a unique function (Equation 14) over the whole image.

5.2 Camera calibration

From Figure 8 can be inferred that undistorted image coordinates (u_i,v_i) can be derived by application of the corrections to the observed ones. With the corrected values, the camera parameters can be determined using the linear approach presented in section 2. Table 2 illustrates the results obtained in function of the number of control points used the computation. It illustrates also that accuracy and stability is ensured with a large number of well distributed control points.

Table 2: camera parameters in function of control point

Number of Points / Parameters	8	100	200	300	339
r_{11}	0.8913	0.8959	0.8922	0.8936	0.8941
r_{12}	0.0142	0.0138	0.0135	0.0140	0.0140
r_{13}	-0.4531	-0.4441	-0.4515	-0.4487	-0.4484
r_{21}	-0.0044	-0.0050	-0.0050	-0.0043	-0.0043
r_{22}	-0.9991	-0.9990	-0.9991	-0.9991	-0.9991
r_{23}	-0.0408	-0.0435	-0.0428	-0.0412	-0.0411
r_{31}	-0.4534	-0.4443	-0.4516	-0.4489	-0.4476
r_{32}	0.0384	0.0412	0.0405	0.0387	0.0387
r_{33}	-0.8905	-0.8949	-0.8913	-0.8928	-0.8933
t_x [m]	-0.8549	-0.9327	-0.8813	-0.9189	-0.9229
t_y [m]	-1.9553	-1.9940	-1.9822	-1.9633	-1.9621
t_z [m]	8.4936	8.5744	8.5719	8.6312	8.6302
u_0 [pix]	1466.8873	1448.2182	1454.7787	1463.8125	1463.9584
v_0 [pix]	2255.3005	2291.3934	2269.6945	2287.5276	2287.5727
α_u [pix]	3565.7579	3641.3738	3635.4077	3658.2736	3657.8602
α_v [pix]	3567.3393	3620.5176	3624.6814	3648.1199	3647.9689

6- Discussion and Conclusion

A procedure and mathematical model have been developed to address new developments, possibilities and challenges in the field of photogrammetry, as a consequence of the tremendous expansion in the digital camera market. One of the challenges lies in finding proper ways, for potential photogrammetry practitioners, to deal efficiently with the optical mechanical characteristics of these cameras.

This paper addresses that challenge. It presents the camera calibration technique developed at ... The complete procedure, described in the paper, has been implemented in Matlab, and can be used to compute these essential elements that are the camera parameters and lens distortions.

In the procedure that has been developed, subpixel accuracy is obtained in the extraction of control-points image coordinates. There are two steps in the operation. First, the edge points in the image are found using a *Hough transform*. Then, image coordinates of control points are determined by applying a least squares solution to the ellipse model (Equation 19).

A new model for lens distortion has been introduced, in which the parameters control the more complex forms of the new cameras. A Composed Cubic Splines function has replaced the polynomial expressions which generally describe radial and tangential distortions. With this approach, it is possible to take into account the interpolation error, which is not negligible, sometimes, compared to distortion correction. With the new method, the residuals at control points are always zeroed.

The efficiency of this model and the quality of the results have led to its implementation as the current camera calibration procedure at Metrology Laboratory, Department of Geomatic Sciences, Université Laval.

References

Ballard D.H. 1981. Generalizing the Hough Transform to Detect Arbitrary Shapes, *Pattern Recogniton*, No 2, pp. 111-122.

Brand, P., R. Mohr, and Ph. Bobet. 1993. Optical distorsions: correction in a projective model, *INRIA*, issn 0249-6399.

Cramer, M. 2004. EUROSDR Network on Digital Camera Calibration. *International Archives of Photogrammetry Remote Sensing and Spatial Information Sciences*. Vol 35, pp. 204-209.

Faugeras, O. and G. Toscani. 1987. Camera calibration for 3D computer Vision. *Proc. of International Workshop on Machine Vision and Machine Intelligence*, pp. 240-247.

Ha, J. and D. Kang. 2005. Initialization method for self-calibration using 2-views. *Pattern recognition*, Vol. 38, No 1, pp. 143-150.

Ma L., Y. Chen, and K.L. Moore. 2003. A New Analytical Radial distorsion Model for camera calibration, *CoRR cs.CV/0307046 (2003)*.

Mateos, G.G. 2000. A Camera Calibration Technique Using Targets of Circular Features. *5th Ibero-America Symposium On Pattern Recognition (SIARP)*.

Perse, J. and S. Kovacic, 2002. Nonparametric, model-based radial lens distortion correction using tilted camera assumption. *Proceedings of the Computer Vision Winter Workshop 2002*, pp. 286–295.

Plante F. 1999. Rétroingénierie de surfaces complexes continues à l'aide des splines cubiques composées et de la décomposition triangulaire, pp.30-74, Thèse de doctorat, Université Laval.

Ramalingam, S., P. Sturm, and S.K. Lodha. 2005. Towards complete generic camera calibration. *Conference on Computer Vision and Pattern Recognition*, San Diego, USA, pp. 1093–1098.

Tsaï, R. 1987. A versatile camera calibration technique for high-accuracy 3D machine vision metrology using off-the-shelf TV cameras and lenses. *IEEE Journal of Robotics and Automation*, vol. 3, No 4, pp. 323-344.

Weng, J., P. Cohen, and M. Herniou, 1990. Calibration of stereo cameras using a non-linear distortion model. *International Conference on Computer Vision and Pattern Recognition*, pp. 246-253.

Weng, J., P. Cohen, and M. Herniou. 1992. Camera Calibration with Distortion Models and Accuracy Evaluation. *IEEE Trans. Pattern Analysis and Machine Intelligence*, Vol. 14, No. 10, pp. 965-980.

Zhang, H., G. Zhang, and W. K-Y Kenneth. 2005. Camera calibration with spheres: linear approaches *Proc. of IEEE International Conf. on Computer Vision*, pp. 782–789.

Zhang, Z., M. Li, K. Huang, and T. Tan. 2008. Practical camera auto-calibration based on object appearance and motion for traffic scene visual surveillance. *Proceedings of IEEE Conference on CVPR.*

Zollener, H. 2003. A Calibration Technique for CCD Cameras using Pose Estimation. *Pattern Recognition and Image Processing Group*, Vol 179, pp 237-244.